Identification of Unfolding Domains in Large Proteins by Their Unfolding Rates†

Yuzhong Deng and David L. Smith*

Department of Chemistry, University of Nebraska-Lincoln, Lincoln, Nebraska 68588-0304

Received November 3, 1997; Revised Manuscript Received February 25, 1998

ABSTRACT: Three unfolding domains in rabbit muscle aldolase destabilized in 3 M urea have been identified from their unfolding rate constants (0.10, 0.036, and 0.0064 min^{-1}). The populations of folded and various, partially unfolded forms were determined by amide hydrogen exchange and mass spectrometry. Results of this study show that unfolding domains may include multiple, noncontiguous segments of the backbone and that different regions of helices may belong to different unfolding domains. In addition, these results show that the domain unfolding most rapidly is located distant from the subunit binding surfaces and has the greatest access to the denaturant. The bimodal intermolecular distributions of deuterium found in this study show that unfolding of these domains is cooperative. It is proposed that these unfolding domains are correlated with local energy minima in the free-energy folding surface of aldolase. In addition to the three unfolding domains, there are three short segments that do not unfold in 3 M urea. These segments, which are located in the subunit binding surface, identify the most stable regions of aldolase. This study also demonstrates that it is now possible to identify and characterize unfolding domains in relatively large (M_r 158 000) proteins.

Recent descriptions of protein folding invoke a multitude of parallel microscopic paths along the folding surface describing the free energy of each conformation (*1*, *2*). These folding surfaces may be smooth or may include free energy barriers that trap transient, partially folded forms of a protein. Characterizing such energy barriers, which will be required for validating any model for protein folding, may be approached via unfolding experiments performed under conditions of thermodynamic equilibrium in which higher energy conformational states are populated according to the Boltzmann distribution (*2*). Bai et al. have used this general approach to probe the unfolding surface of cytochrome *c* (*3*). The present study demonstrates that three high-energy forms of partially unfolded rabbit muscle aldolase (M_r 158 000) can be identified by their characteristic unfolding rates, which were determined by amide hydrogen exchange/mass spectrometry (HD/MS). The intermolecular distribution of deuterium within the entire population of aldolase molecules was determined using the protein fragmentation/MS approach (*4*, *5*). Cooperative localized unfolding of the intact protein incubated in 3 M urea was detected through bimodal isotope patterns in the mass spectra of these peptides. Results of this study provide the first view of localized unfolding in proteins that are much too large to be studied by current NMR methods.

†This study was supported by a grant from the National Institutes of Health (RO1 GM 40384) and by the Nebraska Center for Mass Spectrometry.

* Author to whom correspondence should be addressed. Tel: 402 472-2794; Fax: 402 472-9862. E-mail: DLS@UNLINFO.UNL.EDU.

[1] Abbreviations: ESIMS, electrospray ionization mass spectrometry; Da, dalton; F(H), protiated folded form of protein; H/D, hydrogen/deuterium; HPLC, high-performance liquid chromatography; MS, mass spectrometry; U(D), deuterated unfolded form of protein.

MATERIALS AND METHODS

Rabbit muscle aldolase was equilibrated in 5 mM phosphate/H_2O buffer (pH 6.8, 25 °C) for approximately 1 h, then transferred to a urea/H_2O solution (3 M urea, 5 mM phosphate, pH 6.8, 25 °C), where it was incubated for 3 min to 48 h. The aldolase concentration in this solution was 0.2 mM. Unfolded regions of aldolase were labeled by diluting the solution 20-fold with urea/D_2O buffer (3 M urea, 5 mM phosphate, pH 6.8, 25 °C). Isotopic exchange was quenched after 10 s by decreasing the pH and temperature (pH 2.5, 0 °C). Unlabeled aldolase (0% reference) was prepared by dissolving aldolase in the quench solution (0.1 M phosphate, pH 2.3, 0 °C, 1:1 D_2O/H_2O), while completely exchanged aldolase (100% reference) was prepared by incubating aldolase in D_2O at 37 °C for 3 h at neutral pD followed by a second incubation at pD 2.3 for 3 h. Isotopic exchange was quenched by decreasing the pH and temperature (pH 2.5, 0 °C). Reported pH and PD values were taken directly from the meter without correction. To determine the extent of hydrogen exchange during the incubation time, the samples were digested with pepsin and analyzed by directly coupled HPLC ESIMS using a Micromass Autospec high-resolution mass spectrometer, as described previously (*6*). Approximately 250 pmol of aldolase was used for each incubation time.

The unfolding of aldolase in 3 M urea was detected by near UV (275 nm) and far UV (222 nm) circular dichroism using a Jasco J-600 spectrophotometer. The unfolding of aldolase, as monitored by CD at 222 nm, proceeds with a single smooth transition, suggesting that unfolding is complete in 8 M urea. Measurements made at 0 and 8 M urea were used to determine the extent of unfolding in 3 M urea. The aldolase concentration was 5 μM.

S0006-2960(97)02711-6 CCC: $15.00
Published on Web 04/15/1998

RESULTS

Detecting Localized Unfolding by Hydrogen Exchange/MS. The localized unfolding model for amide hydrogen exchange, illustrated in eq 1, forms the basis for detecting partially unfolded intermediates by HD/MS (*7, 8*). Kinetics for localized unfolding, refolding, and isotope exchange from unfolded forms are described by rate constants k_1, k_{-1}, and k_2.

$$\mathrm{F(H)} \underset{k_{-1}}{\overset{k_1}{\rightleftharpoons}} \mathrm{U(H)} \xrightarrow[\mathrm{D_2O}]{k_2} \mathrm{U(D)} \underset{k_1}{\overset{k_{-1}}{\rightleftharpoons}} \mathrm{F(D)} \qquad (1)$$

Isotope exchange in the folded protein, F(H), is usually much slower than in the unfolded polypeptide because hydrogens located at peptide amide linkages may be hydrogen bonded to other regions or they may be shielded from the deuterated solution. Isotope-exchange rates increase dramatically, often by several orders of magnitude, as proteins unfold. For the experimental conditions used in this study (pH 6.8, 25 °C), isotope exchange from unfolded regions was complete within 10 s (*9*).

The phenomenological rate constant for isotope exchange, k_{ex} is related to k_1, k_{-1}, and k_2, as indicated in eq 2. When the refolding rate is much greater than the isotope exchange rate ($k_{-1} \gg k_2$),

$$k_{ex} = (k_1 k_2)/(k_{-1} + k_2) \qquad (2)$$

a region unfolds and refolds many times before isotope exchange is complete at all peptide linkages in this region. This kinetic limit [EX2 kinetics (*7, 8, 10*)] leads to random distribution of deuterium in the unfolding region among all molecules comprising a sample. Mass spectra of peptides derived from regions in which deuterium is distributed randomly among all molecules exhibit one envelope of isotope peaks. When the refolding rate is much less than the isotope-exchange rate ($k_{-1} \ll k_2$), a region becomes completely deuterated the first time it unfolds (EX1 kinetics). Mass spectra of peptides derived from unfolding regions may exhibit two envelopes of isotope peaks (*5, 11, 12*).

Amide hydrogen-exchange rates averaged over all peptide amide linkages have been determined for several small, intact peptides and proteins by mass spectrometry (*11*−*15*). In addition, methods for measuring localized hydrogen-exchange rates, originally developed for tritium (*16, 17*), have been adapted for mass spectrometry (*4, 5*). The protein fragmentation/MS approach, which relies on proteolytic fragmentation of a protein following a period of isotopic exchange, has been used to determine H/D exchange in several small proteins (*6, 18*−*21*), as well as in large proteins, including aldolase (M_r 158 000) (*12, 22*) and α-crystallin (M_r ∼500 000) (*23*).

Unfolding of Aldolase in 3 M Urea. The kinetics of localized unfolding of aldolase in 3 M urea were investigated by incubating the protein in urea/H_2O for various times, pulse labeling the protein with deuterium (urea/D_2O) for 10 s, acidifying to quench isotope exchange, fragmenting with pepsin, and analyzing by HPLC ESIMS. Unfolded regions of aldolase were expected to be completely deuterated; folded regions were expected to have little or no deuterium. Experimental ESIMS isotope patterns found for the segment including residues 257−269 of aldolase incubated in urea/H_2O for various times illustrate isotope patterns characteristic of hydrogen exchange via the EX1 kinetic limit (Figure 1, panels B−E). The two envelopes of isotope peaks found for this segment following incubation of aldolase in 3 M urea for 10−480 min indicate a bimodal, intermolecular distribution of deuterium in the region including residues 257−269.

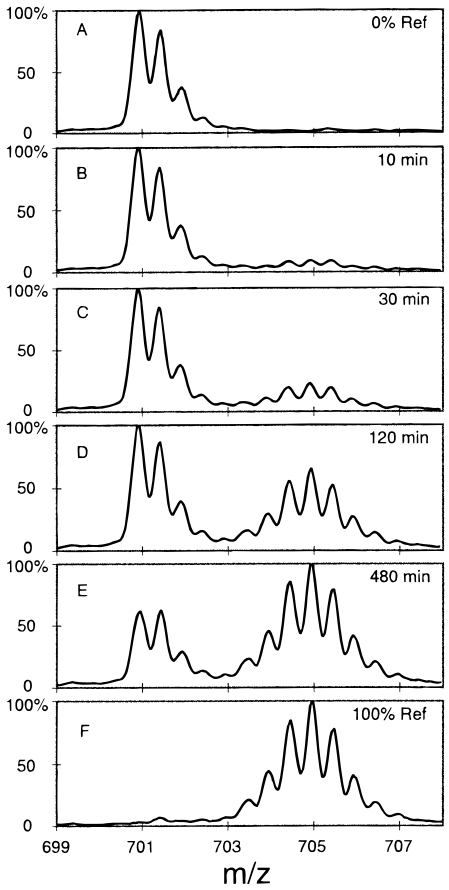

FIGURE 1: ESI mass spectra of the doubly charged peptide including residues 257−269 of aldolase derived from the intact protein, which was incubated in 3 M urea/H_2O for 10−480 min, then pulse labeled for 10 s in 3 M urea/D_2O (panels B−E). Mass spectra for the same segment of aldolase that contained no deuterium or was completely exchanged in D_2O are presented in panels A and F, respectively.

The isotope pattern in Figure 1A was obtained for this segment when taken from aldolase that was not incubated in D_2O, while the pattern in Figure 1F is for the same segment taken from aldolase in which all exchangeable hydrogens had been replaced with deuterium. The difference in the average molecular masses of this peptide derived from the two reference samples of aldolase, 7.8 Da, indicates the number of deuteriums present when the peptide reached the mass spectrometer. Since the HPLC step was performed in H_2O, rapidly exchanging deuterium located on the side chains was replaced with protium before the peptides reached the mass spectrometer (*9*). Although the digestion and HPLC conditions have been chosen to minimize isotope exchange during analysis, some exchange did occur at this time. The extent of this artifactitious exchange was determined from reference spectra for each peptide. For example, this segment has 12 peptide linkages, two of which are proline. Hence, it has 10 peptide amide hydrogens. Finding 7.8 deuteriums in this segment of completely exchanged aldolase indicates 78% recovery of deuterium. A procedure used to

adjust for deuterium loss during analysis has been described (*4*).

Deuterium levels in the reference peaks for segment 257−269 (Figure 1, panels A and F) were used to determine the extent to which a subpopulation of aldolase was unfolded in the region including residues 257−269 of the intact protein when incubated in 3 M urea for various times. The average mass of peptides represented by the high mass envelope (Figure 1, panels B−E) is the same as the average mass of peptides derived from aldolase in which all exchangeable hydrogens had been replaced with deuterium (Figure 1F). This result indicates that the region including residues 257−269 was completely unfolded, as sensed by hydrogen exchange, in a subpopulation of aldolase molecules during the brief labeling step. Similarly, the average mass of peptides represented by the low mass envelope (Figure 1, panels B−E) is approximately equal to that of the average mass of the same peptide derived from aldolase that was not incubated in D_2O, suggesting that this region was completely folded in the remaining population of aldolase molecules. It is noted that the average mass of peptides derived from folded aldolase molecules increased slightly with incubation time, as indicated by the increasing relative intensity of the second peak in the low mass envelope (Figure, panels B−E). This small, but measurable level of deuterium in peptides derived from aldolase that was folded in this region is due to hydrogen exchange occurring through processes other than EX1 kinetics. These processes may include exchange directly from the folded state (*24*, *25*) as well as exchange from short-lived, partially unfolded states (i.e., EX2 kinetics) (*8*).

It is also important to note that finding nearly all of the signal in either the low or the high mass envelopes (Figure 1, panels B−E) is direct evidence that the region including residues 257−269 of all aldolase molecules in the sample was either completely folded or completely unfolded. Molecules partially unfolded in this region are expected to undergo incomplete exchange, which would be detected as intensity in the mass range between the two envelopes. The present results clearly indicate that this region unfolds in most aldolase molecules by a one-step cooperative process. The relative intensities of the two envelopes are a direct measure of the relative number of aldolase molecules in which the segment including residues 257−269 was folded or unfolded. For example, the relative intensities of isotope envelopes found for peptides derived from the 257−269 segment of aldolase indicate that 43% of aldolase was unfolded in this region following incubation of the intact protein in 3 M urea for 2 h (Figure 1D).

Rate Constants for Localized Unfolding. The procedures for pulse labeling and analysis described above for the segment including residues 257−269 were used to investigate localized unfolding of aldolase following incubation of the intact protein in 3 M urea for 3 min to 48 h. Thirty-two peptic fragments representing approximately 70% of the entire backbone were used in this study. The ESI mass spectra of 29 of these peptides had bimodal isotope patterns (as in Figure 1, panels B−E), suggesting bimodal, intermolecular distributions of deuterium in the corresponding segments of the aldolase backbone. The populations of aldolase folded and unfolded in a particular region, as indicated by the areas of the low and high mass envelopes,

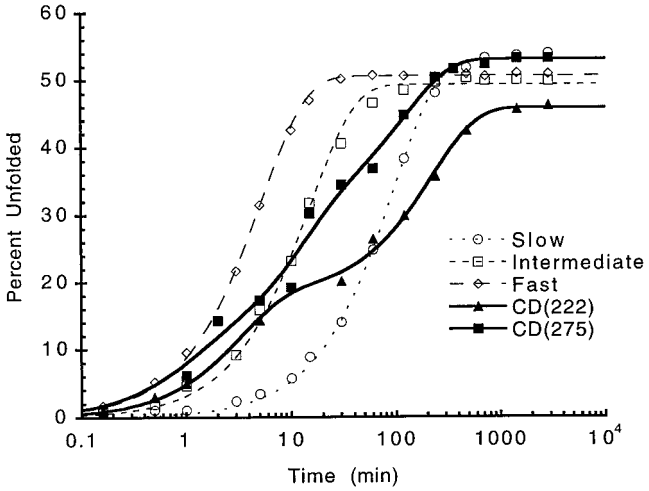

FIGURE 2: Dashed lines indicate the fraction of the entire aldolase population that was unfolded in short segments defined by peptic fragmentation of the aldolase backbone following incubation of aldolase in 3 M urea for 3 min to 48 h. Unfolded regions were labeled with deuterium by pulse labeling for 10 s. Results for the 27 fragments listed in Table 1 have been combined into three groups (Slow, $k_1 = 0.0064$ min^{-1}; Intermediate, $k_1 = 0.036$ min^{-1}; Fast, $k_1 = 0.10$ min^{-1}) as described in the text. The losses of α-helix and tertiary structure, determined by CD at 222 and 275 nm, respectively, of aldolase in 3 M urea are indicated by solid lines.

were estimated by fitting the reference spectra to the bimodal spectra to achieve the best fit. A computer program has been written for this simulation (*26*). Analysis of 27 peptides led to a compilation of the percentage of aldolase that was unfolded in regions represented by these peptides following incubation of the intact protein in 3 M urea for various times. These results are summarized in Figure 2 and Table 1.

Preliminary analysis showed that 20−500 min were required for the fraction of aldolase that was unfolded in these regions to reach a steady state. This is the time required to establish equilibrium populations of the folded form with various unfolded forms. Closer analysis of the results indicated that the rates at which different segments of the aldolase backbone approached the equilibrium population fall into three groups whose unfolded populations are represented by the dashed lines in Figure 2. The data points represent the mean for all peptides in each of the three groups. Rate constants describing unfolding of regions represented by these 27 peptides (k_1 of eq 1) were determined by fitting model parameters (see Appendix) to the experimental results presented in Figure 2. Analysis of the combined data indicate that regions represented by these three groups of peptides unfold in 3 M urea with rate constants of 0.10, 0.036, and 0.0064 min^{-1}. Unfolding rate constants for individual peptides are presented in Table 1 to identify the segments comprising the three groups and to illustrate the uniqueness of the three unfolding groups. The precision with which the unfolding rate constants were determined by this approach is indicated by results for three overlapping segments that include residues 255−269, 256−269, and 257−269. As indicated in Table 1, the rate constants for unfolding of this region were 0.0069 ± 0.0002 min^{-1}.

Unfolding Detected by CD. Circular dichroism spectroscopy at 222 and 275 nm has been used to follow the loss of α-helix and tertiary structure of aldolase in 3 M urea (Figure 2). The percent of aldolase that remained folded after

Table 1: Rate Constants for Unfolding of 27 Segments of Rabbit Muscle Aldolase Incubated in 3 M Urea at 25 °C and pH 6.8[a]

slow			intermediate			fast		
segment[b]	k_{unf}[c]	exposure[d]	segment[b]	k_{unf}[c]	exposure[d]	segment[b]	k_{unf}[c]	exposure[d]
1−17	0.0051	61	41−49	0.033	74	58−64	0.10	13
152−161	0.0077	43	116−127	0.032	24	68−78	0.10	23
152−162	0.0077	39	124−131	0.029	20	79−83	0.10	35
171−177	0.0063	6	144−151	0.043	14	84−105	0.11	44
178−187	0.0055	13	148−151	0.041	25	299−307	0.11	9
180−187	0.0051	6	229−238	0.042	26	311−320	0.10	73
255−269	0.0069	8	247−250	0.029	45	311−326	0.10	70
256−269	0.0068	8	280−283	0.041	8	327−336	0.09	28
257−269	0.0071	9	284−298	0.043	40	357−363	0.10	157
mean	0.0064	21	mean	0.036	31	mean	0.10	50
std dev	0.0010		std dev	0.007		std dev	0.008	

[a] The solvent exposure, normalized to the number of residues in each segment, is also given for each segment. Two segments (see Figure 3) that include parts of two unfolding domains, as well as three segments in which unfolding in 3 M urea was too slow to measure are not included. [b] Residues of peptic fragments. [c] Units of inverse minutes. [d] Solvent exposure per residue in units of Å^2 (*27, 39, 40*).

incubation in 3 M urea for various times was calculated from CD signals obtained for native aldolase and aldolase that was completely unfolded in 8 M urea. Results for loss of α-helix structure were fitted to a kinetic expression using two exponential terms, giving apparent unfolding rate constants of 0.3 and 0.004 min^{-1}. These results demonstrate that the time frames for unfolding of aldolase in 3 M urea are similar when sensed by either CD or hydrogen exchange. However, since the CD results are averaged over all regions of the aldolase structure and over the entire population, while the hydrogen exchange gives both the extent of unfolding in specific regions as well as the corresponding populations, a more quantitative comparison between CD and hydrogen exchange seems unwarranted.

DISCUSSION

Rabbit muscle aldolase (d-fructose-1,6-bisphosphate D-glyceraldehyde-3-phosphate-lyase) is a class 1 aldolase with eight β-strands linked by α-helices to form a classic parallel β-barrel (*27*−*29*). The active protein is a homotetramer in which each subunit has 363 residues and a relative molecular mass of 39 000 Da. The high stability of the quaternary structure of aldolase precludes dissociation into subunits at the concentrations used in this study (*30*). Aldolase has been used as a model to investigate energy barriers in the folding surfaces of large proteins because it is a relatively well-behaved protein that undergoes reversible unfolding and refolding (*31, 32*) and because its structure and function have been studied extensively (*33*). This study differs from many previous studies of the unfolding of large proteins in that unfolding domains have been identified and their unfolding rates have been determined. Although traditional methods for detecting protein unfolding, such as UV absorbance, CD spectroscopy, tryptophan fluorescence, and calorimetry, may indicate the presence of multiple unfolding domains, they generally cannot be used to identify the unfolding domains. Unfolding of a few small proteins has been investigated by hydrogen exchange/NMR (*3, 25, 34, 35*), but there appears to be no reports of previous studies in which unfolding domains of large proteins were identified and characterized by their unfolding rates.

In the present study, 27 peptic fragments of aldolase displayed bimodal isotope patterns consistent with H/D exchange occurring through EX1 kinetics and cooperative unfolding. The fraction of the aldolase population that was unfolded in regions represented by these 27 peptides was determined from the relative abundances of the isotope envelopes (Figure 1) as a function of the time aldolase was incubated in urea. The unfolding rates of the backbone regions represented by these peptides fell into three groups, designated as Slow, Intermediate, and Fast in Figure 2 and Table 1. The locations of these cooperative unfolding segments with respect to the primary and secondary structures of aldolase are illustrated in Figure 3, while the locations of these units in the tertiary structure of the aldolase monomer are depicted in Figure 4. Although much of the C-terminal region, starting approximately from residue 300, belongs to the Fast unfolding domain, segments belonging to all three unfolding domains were found throughout the remainder of the backbone. These results show that unfolding domains may include multiple, noncontiguous segments of the backbone. In addition to the 27 segments described above, two additional segments (including residues 18−30 and 199−214) displayed bimodal isotope patterns, but the deuterium level indicated by the high mass envelope was less than 100%. This behavior is expected for segments spanning two domains with different unfolding rates.

Several pairs of peptides (e.g., 116−127/124−131, 144−151/148−151, and 311−320/311−326) derived from overlapping regions of the backbone have the same unfolding rates. These results show that the region represented by each pair of peptides unfolds cooperatively. Although there are only a few regions for which such direct evidence for cooperative unfolding extending beyond the segments indicated in Figure 3 exists, it is likely that all regions of the backbone represented by segments exhibiting similar unfolding rates undergo cooperative unfolding. The large differences among the mean unfolding rates of the three groups versus the standard deviation of the folding rates within the groups supports the existence of three unfolding domains. Unfolding of any of these domains leads to a partially unfolded form of aldolase that presumably correlates with an energy barrier on the free-energy folding surface (*2*).

In addition to the 29 fragments displaying bimodal isotope patterns, three segments (residues 166−170, 203−206, and 251−255) displayed a single envelope isotope pattern. These segments, located in α-helices *D*, *E*$_1$, and *F*, were designated

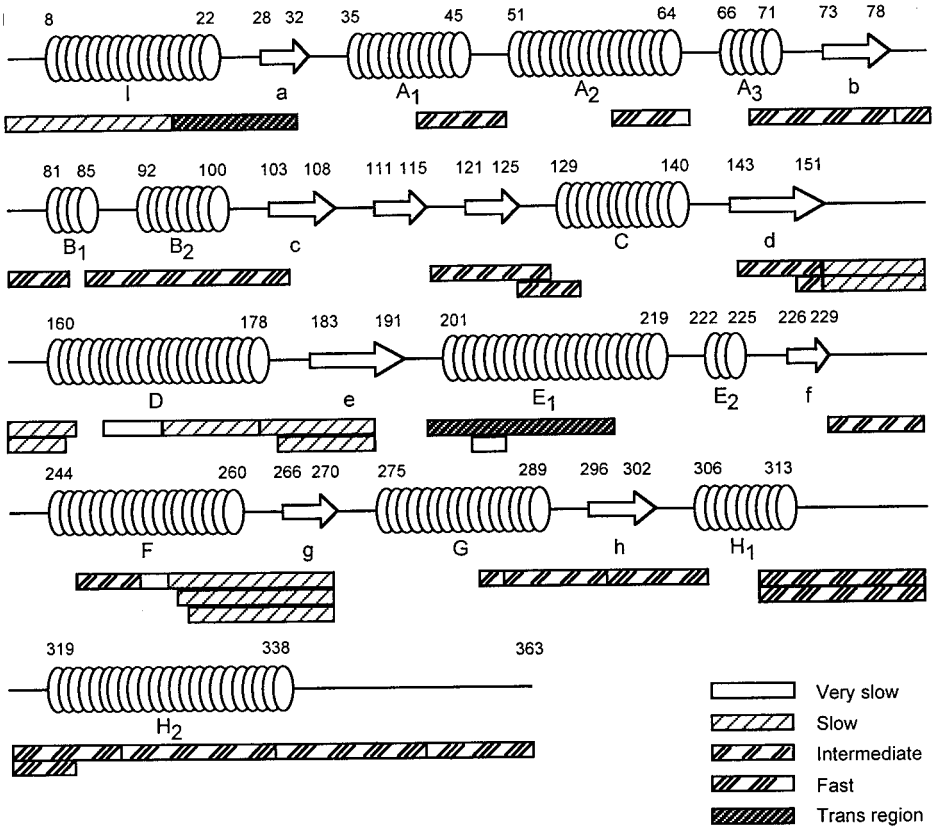

FIGURE 3: Locations of the three unfolding domains with respect to the primary and secondary structures of aldolase. α-Helices (coils) and *β*-strands (arrows) are drawn to scale. The loop regions, which are indicated by solid lines are not drawn to scale. Secondary structure is based on the X-ray diffraction structure of human aldolase, which is highly homologous to rabbit muscle aldolase (*27, 29)*. The elements of secondary structure are labeled according to the scheme used by Sygusch et al. (*28)*.

as Very Slow in Figure 3. The deuterium levels of these segments were barely detectable, indicating that these segments were tightly folded in the entire aldolase population, even after equilibration in 3 M urea for 48 h. All three segments were derived from interior regions of α-helices, consistent with previous reports of increased stability of the interiors of some α-helices in lysozyme (*36*).

The results presented in Figure 3 also suggest that the boundaries for the unfolding domains are not highly correlated with the secondary structural elements of aldolase. For example, the N-terminal region of the F α-helix belongs to the Intermediate unfolding domain, the C-terminal region of the same α-helix belongs to the Slow unfolding domain, and the interior region belongs to the Very Slow unfolding domain. Similar analysis of unfolding in other elements of secondary structure indicates that α-helices I, D, and E1, as well as *β*-strand h, contain regions belonging to different unfolding domains. It is evident from these results that elements of secondary structure may transcend the boundaries of the unfolding domains.

Peptic fragments comprising the three unfolding domains are located with respect to the tertiary and quaternary structures of aldolase in Figure 5. Unfolding domains designated as Very Slow, Slow, Intermediate and Fast are indicated by black, magenta, yellow, and red, respectively. Transitions regions between the unfolding domains, as well as regions for which peptic fragments were not found are indicated by gray. This presentation clearly shows that rapidly unfolding regions of aldolase equilibrated in 3 M urea are located most distant from the subunit binding surface, while slowly unfolding regions are located along the subunit binding surface.

Each aldolase subunit contacts two other subunits (*29*). The more extensive of the subunit binding surfaces involves interactions of the side chains from α-helices *E* and *F* from adjacent subunits, while the less extensive of the subunit binding surfaces involves α-helix *D*. The α-helices are labeled in Figures 3 and 4. The three segments whose unfolding rates in 3 M urea were too slow to be measured (black in Figure 5) are located in these α-helices, which have a primary role in subunit binding. This presentation indicates that the two segments located in α-helices E and F (residues 203−206 and 251−255) directly contact the corresponding segments in the adjacent aldolase subunit. The other very stable segment, located in α-helix D, is near, but perhaps not in direct contact with the same segment in the other adjacent subunit. Alternatively, the contact regions of adjacent D helices may not be the same in the crystal as in solution. The extreme stability of these regions, indicated by their low H/D exchange rates, is consistent with the size exclusion chromatography results, which indicated that aldolase exists as a tetramer in 3 M urea (data not shown).

Results presented in Figures 3 and 5 show that unfolding domains of aldolase incubated in 3 M urea are better defined in terms of tertiary and quaternary structure than in terms of primary or secondary structure. Estimates of the access these domains have to the surface of aldolase are presented in Table 1. For aldolase equilibrated in 3 M urea, the region most distant from the subunit binding surface has the greatest

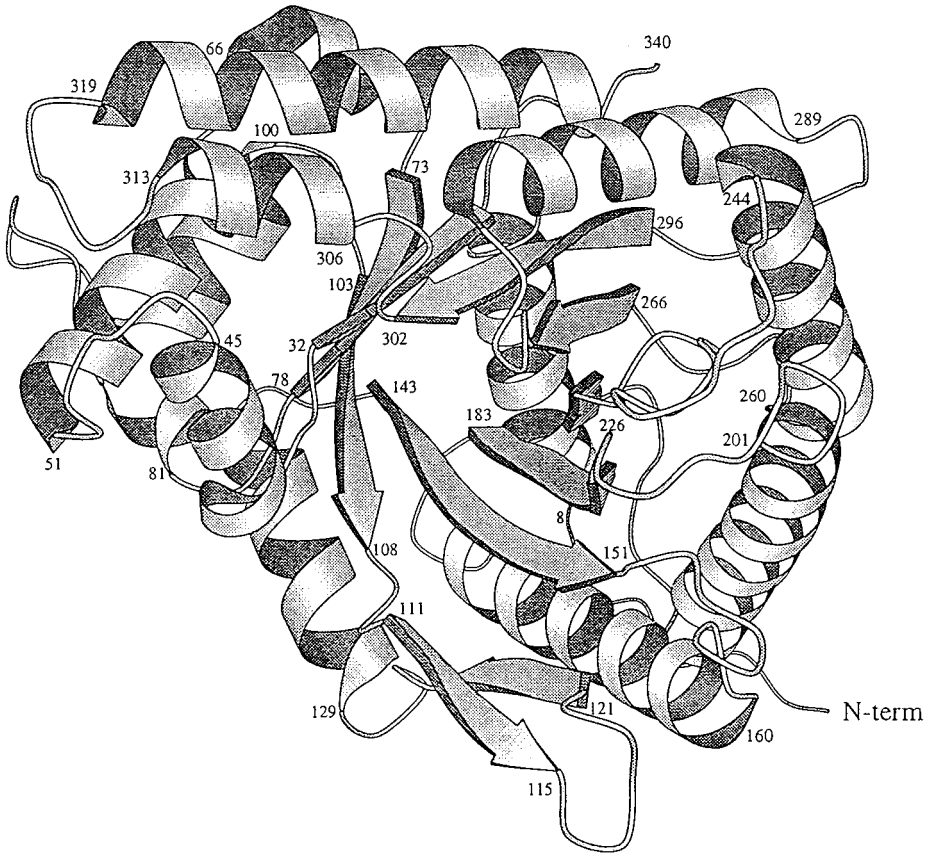

FIGURE 4: Three-dimensional structure of the aldolase monomer which may be used to locate units of secondary structure and unfolding domains described in Figure 3 [Drawn using Molescript (*41)* and adapted from ref. *12*].

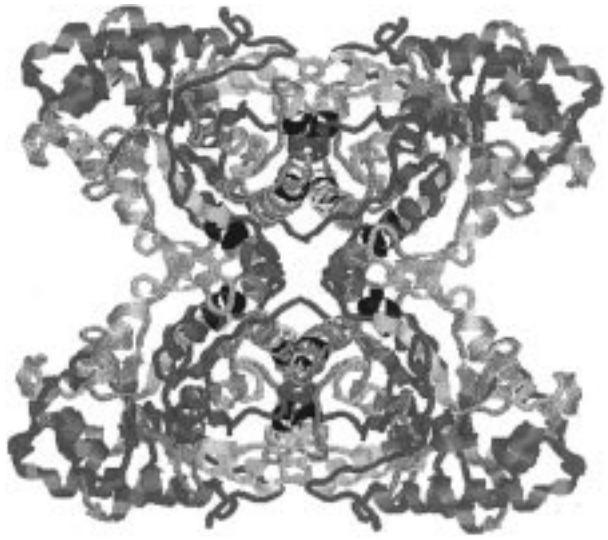

FIGURE 5: Tetramer structure of aldolase illustrating locations of unfolding domains exhibiting Very Slow (black), Slow (magenta), Intermediate (yellow) and Fast (red) unfolding in 3 M urea. Transition regions, as well as regions for which fragments were not found are indicated in gray.

exposure to the aqueous/urea solution (50 Å^2) and unfolds with a half-life of 6.9 min (Fast unfolding domain). Another unfolding domain, which is located between this domain and the domain adjacent to the subunit binding surface, has less exposure to the aqueous/urea solution (31 Å^2) and unfolds with a half-life of 19 min (Intermediate unfolding domain). The domain located closest to the subunit binding surface has the least exposure to the aqueous/urea solution (21 Å^2) and unfolds with a half-life of 108 min (Slow unfolding domain). The three short segments in α-helices D, E, and F most important for holding the subunits together in 3 M urea are not included in the three unfolding domains. With an average exposed surface of only 9 Å^2, these segments have very little access to the aqueous/urea solution. Given the relative locations of the three unfolding domains in the tertiary structure of aldolase, it seems likely that the domain defined by the Intermediate unfolding rate unfolds either with or after unfolding of the Fast domain. Likewise, it seems likely that the Slow domain unfolds either with or after unfolding of both the Fast and Intermediate domains.

Bai et al. have shown that unfolding domains can be identified from their free energies by increasing the populations of unfolded forms by either using denaturants to stabilize the unfolded forms or by raising the temperature (*37*). A previous study of the thermal-induced unfolding of aldolase (*22*) demonstrated little evidence for H/D exchange via the EX1 mechanism. In the present study of urea induced unfolding, H/D exchange occurs almost entirely by the EX1 mechanism. Thus, urea and high temperature have profound effects on the dynamics of protein unfolding. Urea dramatically decreases the rate of refolding (k_{-1}) but has much less effect on the intrinsic rate (k_2) of hydrogen exchange (*38*), whereas, increasing the temperature increases both k_{-1} and k_2 such that k_2 is never greater than k_{-1}. Results of the thermal-induced unfolding study show that the region located most distant from the subunit binding surface is least stable while the region located along the subunit binding surface is most stable. Thus, high temperature or urea affect the hydrogen exchange dynamics differently, but have similar effects on aldolase unfolding.

ACKNOWLEDGMENT

The authors are pleased to acknowledge discussions with C. M. Dobson and S. W. Englander, P.-S. Song for use of his CD spectrophotometer, and assistance from Z. Zhang during the early stages of the study.

APPENDIX

The results in Figure 2 show the rates at which equilibrium populations of folded and different, partially unfolded forms of aldolase was established. The differential rate expression for the concentrations of folded, [F], and unfolded, [U], was integrated to give the following expression:

$$[U] = [K_{unf}/(K_{unf} + 1)][1 - \exp(-k_1(K_{unf} + 1)/K_{unf})t]$$

Rate constants for unfolding in each segment, k_1, were determined by fitting this expression to the experimental data. The unfolding equilibrium constant, K_{unf}, was determined from the steady-state populations of folded and unfolded forms.

REFERENCES

1. Baldwin, R. L. (1995) *J. Biomol. NMR 5*, 103−109.
2. Dill, K. A., and Chan, H. S. (1997) *Nat. Struct. Biol. 4*, 10−19.
3. Bai, Y., Sosnick, T. R., Mayne, L., and Englander, S. W. (1995) *Science 269*, 192−197.
4. Zhang, Z., and Smith, D. L. (1993) *Protein Sci. 2*, 522−531.
5. Smith, D. L., Deng, Y., and Zhang, Z. (1997) *J. Mass Spectrom. 32*, 135−146.
6. Engen, J., Smithgall, T., Gmeiner, W., and Smith, D. L. (1997) *Biochemistry 36*, 14384−14391.
7. Hvidt, A., and Nielsen, S. O. (1966) *Adv. Protein Chem. 21*, 287−385.
8. Englander, S. W., and Kallenbach, N. R. (1984) *Q. Rev. Biophys. 16*, 521−655.
9. Bai, Y., Milne, J. S., Mayne, L., and Englander, S. W. (1993) *Proteins: Struct., Funct., Genet. 17*, 75−86.
10. Miller, D. W., and Dill, K. A. (1995) *Protein Sci. 4*, 1860−1873.
11. Miranker, A., Robinson, C. V., Radford, S. E., Aplin, R. T., and Dobson, C. M. (1993) *Science 262*, 896−900.
12. Zhang, Z., Post, C. B., and Smith, D. L. (1996) *Biochemistry 35*, 779−791.
13. Thévenon-Emeric, G., and Smith, D. L. (1991) *Proc. 39th Conf. Mass Spectrom. Allied Topics*; Nashville, TN; pp 1436−1437.
14. Katta, V., and Chait, B. T. (1991) *Rapid Commun. Mass Spectrom. 5*, 214−217.
15. Anderegg, R. J., and Wagner, D. S. (1995) *J. Am. Chem. Soc. 117*, 1374−1377.
16. Rosa, J. J., and Richards, F. M. (1979) *J. Mol. Biol. 133*, 399−416.
17. Englander, J. J., Rogero, J. R., and Englander, S. W. (1985) *Anal. Biochem. 147*, 234−244.
18. Johnson, R. S., and Walsh, K. A. (1994) *Protein Sci. 3*, 2411−2418.
19. Jaquinod, M., Guy, P., Halgand, F., Caffrey, M., Fitch, J., Cusanovich, M., and Forest, E. (1996) *FEBS Lett. 380*, 44−48.
20. Dharmasiri, K., and Smith, D. L. (1996) *Anal. Chem. 68*, 2340−2344.
21. Yang, H. H., and Smith, D. L. (1997) *Biochemistry 36*, 14992−14999.
22. Zhang, Z., and Smith, D. L. (1996) *Protein Sci. 5*, 1282−1289.
23. Liu, Y., and Smith, D. L. (1994) *J. Am. Soc. Mass Spectrom. 5*, 19−28.
24. Woodward, C., Simon, I., and Tüchsen, E. (1982) *Mol. Cell. Biochem. 48*, 135−160.
25. Kim, K.-S., and Woodward, C. (1993) *Biochemistry 32*, 9609−9613.
26. Zhang, Z. Unpublished Results.
27. Bernstein, F. C., Koetzle, T. F., Williams, G. J. B., Meyer, J., E. F., Brice, M. D., Rodgers, J. R., Kennard, O., Shimanouchi, T., and Tasumi, M. (1977) *J. Mol. Biol. 112*, 535−542.
28. Sygusch, J., Beaudry, D., and Allaire, M. (1987) *Proc. Natl. Acad. Sci. U.S.A. 84*, 7846−7850.
29. Gamblin, S. J., Cooper, B., Millar, J. R., Davies, G. J., Littlechild, J. A., and Watson, H. C. (1990) *FEBS Lett. 262*, 282−286.
30. Beernink, P. T., and Tolan, D. R. (1996) *Proc. Natl. Acad. Sci. U.S.A. 93*, 5374−5379.
31. Stellwagen, E., and Schachman, H. K. (1962) *Biochemistry 1*, 1056−1068.
32. Deal, W. C., Rutter, W. J., and Van Holde, K. E. (1963) *Biochemistry 2*, 246−251.
33. Gefflaut, T., Blonski, C., Perie, J., and Willson, M. (1995) *Prog. Biophys. Mol. Biol. 63*, 301−340.
34. Mayo, S. L., and Baldwin, R. L. (1993) *Science 262*, 873−876.
35. Kiefhaber, T., and Baldwin, R. L. (1995) *Proc. Natl. Acad. Sci. U.S.A. 92*, 2657−2661.
36. Radford, S. E., Buck, M., Topping, K. D., Dobson, C. M., and Evans, P. A. (1992) *Proteins: Struct., Funct., Genet. 14*, 237−248.
37. Bai, Y. W., Milne, J. S., Mayne, L., and Englander, S. W. (1994) *Proteins: Struct., Funct., Genet. 20*, 4−14.
38. Loftus, D., Gbenle, G., Kim, P. S., and Baldwin, R. L. (1986) *Biochemistry 25*, 1428−1436.
39. Blom, N., and Sygusch, J. (1997) *Nat. Struct. Biol. 4*, 36−39.
40. Kabsch, W., and Sander, C. (1983) *Biopolymers 22*, 2577−2637.
41. Kraulis, P. J. (1991) *J. Appl. Crystallogr. 24*, 946−950.

BI972711O